Johann Radon Institute for
Computational and Applied Mathematics
Austrian Academy of Sciences (ÖAW)

# Functional A Posteriori Error Estimates for Discontinuous Galerkin Approximations of Elliptic Problems

R. Lazarov S., S. Tomar

RICAM-Report 2006-40

# FUNCTIONAL A POSTERIORI ERROR ESTIMATES FOR DISCONTINUOUS GALERKIN APPROXIMATIONS OF ELLIPTIC PROBLEMS

RAYTCHO LAZAROV, SERGEY REPIN, AND SATYENDRA TOMAR

Abstract. In this paper, we develop functional a posteriori error estimates for DG approximations of elliptic boundary-value problems. These estimates are based on a certain projection of DG approximations to the respective energy space and functional a posteriori estimates for conforming approximations (see [30, 31]). On these grounds we derive *two-sided guaranteed* and *computable* bounds for the errors in "broken" energy norms. A series of numerical examples presented confirm the efficiency of the estimates.

## 1. Introduction

A posteriori error estimates are intended to (a) give a correct presentation of the overall value of the approximation error and (b) provide a correct indication of the distribution of local errors that can be further used in a mesh adaptation process. A posteriori estimates for conforming approximations of various boundary value problems were in the focus of numerous researches (see, e.g., [1, 6, 7, 9, 15, 17, 27, 28, 38] and the references therein). Typically, the estimates used for finite element approximations were either presented as certain weighted combinations of the element residuals and inter-element jumps (see e.g. [6, 1, 38]) or as the difference between an approximate solution and its post-processed image. The latter method is often motivated by the so called superconvergence phenomenon (see, e.g., [25, 39, 40]).

Though, discontinuous Galerkin methods were initially proposed in 70s-80s (see, e.g., [2, 4, 5] and the references in [3]), they started receiving serious attention much later, and hence, the methods of their a posteriori error control are relatively less investigated. Concerning a posteriori estimates for DG approximations of elliptic type equations we refer to [10, 13, 24], where a residual type estimate for the energy norm of the error was suggested. In [16] a posteriori estimates in $L_2$ norm were derived for the so called "local DG method" applied to an elliptic boundary value problem. Our aproach is close to the method of equlibrated residuals discussed in [1] and recenttly perfected and applied to more general problems in [11]. A posteriori error estimates for DG approximations were also obtained for other classes of problems. In particular, in [19, 21, 22, 37] time-dependent (transport) equations were considered and in [26] a posteriori error estimates for DG approximations of integral equations were obtained.

*Date*: Begin on: December 19, 2005; Today is December 19, 2006.

*Key words and phrases.* a posteriori error estimates, discontinuous Galerkin method, nonconforming approximations.

In this paper, we derive two-sided a posteriori error bounds for DG approximations of an elliptic type problem and investigate their efficiency. Our analysis is based upon the so called functional a posteriori error estimates (see [30, 31, 32, 33, 34] and the book [29]). These estimates are derived on purely functional grounds by the analysis of the respective differential problem. Therefore, they are valid for any conforming approximation and contain no mesh-dependent constants. Moreover, functional error estimates provide *guaranteed* and *computable* upper and lower bounds for any conforming approximation of the exact solution. We exploit these properties in our analysis.

The proposed method for a posteriori error control consists of two steps: (1) a post-processing procedure that maps the DG approximation of the solution to the "energy space" of the problem under considerations, and (2) application of the functional a posteriori estimates to the post-processed solution. The latter requires computing a "free" vector-field (flux) $y$.

For the implementation of both of these steps we propose a number of computational procedures that vary from very cheap (that produce relatively coarse estimates) to more expensive (that practically guarantee effectivity index close to one). The averaging procedures described in Subsections 5.1.1, 5.2.1, and 5.2.2 are simple and cheap. However, if one needs a sharp bound for the error then the procedures suggested in Subsections 5.1.2, and 5.2.3 should be used. Note that the procedures with sharp bound are more expensive, the cost could be comparable with the cost of solving the DG problem itself (see a comparison in Table 9). Nevertheless, all of these procedures provide guaranteed upper bound for the approximation error, which, to the best of our knowledge, lacks from other existing techniques for DG approximations.

Essential part of our paper is Section 6 where we test the proposed procedures for computing a posteriori error bounds on a number of one- and two-dimensional model problems. Our computations, with efectivity indexes below 2 (in the simplest cases it is close to 1), indicate that the proposed methodology is very effective and reliable.

The organisation of this paper is as follows. In Section 2, we present the DG discretization of linear elliptic problems and recall some known results. In Section 3, we briefly discuss functional a posteriori error estimates and their applications to the error estimation of conforming approximations. Functional a posteriori error estimates for DG approximations are derived in Section 4. This is followed by the discussion of various methods to compute the "free" functions arising in the estimates, which is the subject of Section 5. Numerical examples are presented in Section 6.

## 2. DG discretization of elliptic problems

Consider a second order elliptic problem on a bounded Lipschitz domain $\Omega \subset R^d$, $d = 1, 2, 3$:

$$-\nabla \cdot (A(x) \nabla u) = f(x) \qquad \text{in } \Omega, \tag{2.1a}$$

$$u(x) = u_0 \qquad \text{on } \Gamma_D, \tag{2.1b}$$

$$A\nabla u \cdot \mathbf{n} = g_N \qquad \text{on } \Gamma_N. \tag{2.1c}$$

Here $\mathbf{n}$ denotes the exterior unit normal vector to $\partial\Omega \equiv \Gamma$ and $\cdot$ denotes the scalar product of vectors. The boundary is assumed to be decomposed into two disjoint

parts $\Gamma_D$ and $\Gamma_N$. For the DG formulation below we shall need the existence of the traces of $u$ and $A\nabla u\cdot\mathbf{n}$ on the interfaces in $\Omega$, and thus, the solution $u$ is assumed to have the required regularity. It is assumed that $A$ is a symmetric positive definite matrix such that

$$c_1\left|\xi\right|^2 \leqslant A\xi\cdot\xi \leqslant c_2\left|\xi\right|^2 \qquad \forall\xi\in\mathbb{R}^d \tag{2.2}$$

and it has a positive inverse $A^{-1}$. In this case, the norms

$$\|z\|_a^2 = a(z,z) := \int_\Omega Az\cdot z dx,$$
$$\|z\|_{\bar{a}}^2 = \bar{a}(z,z) := \int_\Omega A^{-1}z\cdot z dx$$

are equivalent to the $L^2$ norm $\|z\|$. The respective generalized solution $u$ satisfies the relation

$$\int_\Omega A\nabla u\cdot\nabla w dx = \int_\Omega fw dx, \quad \forall w\in\mathcal{V}_0, \tag{2.3}$$

where

$$\mathcal{V}_0 = \mathcal{V}_0(\mathcal{T}_h) = \{v\in H^1(\Omega) : v = 0 \text{ on } \Gamma_D\}.$$

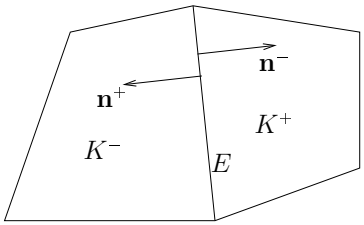


FIGURE 1. Two adjacent finite elements sharing a common face $E$

.

Let $\mathcal{T}_h$ be a non-overlapping partition of $\Omega$ into a finite number of elements $K$. For any $K\in\mathcal{T}_h$ we denote its diameter by $h_K$ and the boundary by $\partial K$. As shown in Figure 1, let $E = \bar{K}^+\cap\bar{K}^-$ be a common face of two adjacent elements $K^+$, and $K^-$. Further, let $h = \max_{K\in\mathcal{T}_h} h_K$ denotes a characteristic mesh size of the whole partition. The set of all the internal faces is denoted by $\mathcal{E}_0$ and $\mathcal{E}_D$ and $\mathcal{E}_N$ contain the faces of finite elements that belongs to $\Gamma_D$ and $\Gamma_N$, respectively. Finally, $\mathcal{E}$ is the set of all the faces: $\mathcal{E} = \mathcal{E}_0\cup\mathcal{E}_D\cup\mathcal{E}_N$. We assume that the partition is quasi uniform, see [35]. We allow finite elements to vary in size and shape for local mesh adaptation and the mesh is not required to be conforming, i.e. elements may possess hanging nodes. Further, the face measure $h_E$ is a quantity defined on each face $E\in\mathcal{E}$ as follows

$$h_E = \begin{cases} |E|, & \text{for } E\in\mathcal{E}, d=2 \\ |E|^{\frac{1}{2}}, & \text{for } E\in\mathcal{E}, d=3 \end{cases}.$$

On the partition $\mathcal{T}_h$ we define a broken Sobolev space:

$$\mathcal{V} := H^2(\mathcal{T}_h) = \{v\in L^2(\Omega) : v|_K\in H^2(K), \forall K\in\mathcal{T}_h\}.$$

Note that the functions in $\mathcal{V}$ **may not satisfy** any boundary condition. By

$$\mathcal{V}_h := \mathcal{V}_h(\mathcal{T}_h) = \{v\in L^2(\Omega) : v|_K\in P_r(K), \forall K\in\mathcal{T}_h\},$$

where $P_r$ is the set of polynomials of degree $r \geqslant 1$, we define a finite dimensional subspace of $\mathcal{V}$. Further, for the vector-valued functions we define the following spaces:

$$\mathcal{Q} := \left(H^2(\mathcal{T}_h)\right)^d = \{\mathbf{q} \in \left(L^2(\Omega)\right)^d : \mathbf{q}|_K \in \left(H^2(K)\right)^d, \forall K \in \mathcal{T}_h\},$$
$$\mathcal{Q}_h := \mathcal{Q}_h(\mathcal{T}_h) = \{\mathbf{q} \in \left(L^2(\Omega)\right)^d : \mathbf{q}|_K \in \left(P_r(K)\right)^d, \forall K \in \mathcal{T}_h\}.$$

On $\mathcal{V}$ we introduce the following forms

$$(A\nabla_h u_h, \nabla_h v_h)_{\mathcal{T}_h} := \sum_{K\in\mathcal{T}_h} \int_K A\nabla_h u_h \cdot \nabla_h v_h dx, \quad \langle p, q\rangle_{\mathcal{F}} := \sum_{E\in\mathcal{F}} \int_E p \cdot q ds,$$

where $\mathcal{F}$ is one of the sets $\mathcal{E}$, $\mathcal{E}_0$, $\mathcal{E}_D$, $\mathcal{E}_N$ or their combinations.

To deal with multivalued traces at the element faces in a DG discretization we introduce some trace operators. We define the *average* ($\{\cdot\}$) and *jump* ($[\![\cdot]\!]$) as follows:
Let $E$ be an interior face shared by elements $K^+$ and $K^-$. Define the unit normal vectors $\mathbf{n}^+$ and $\mathbf{n}^-$ on $E$ pointing exterior to $K^+$ and $K^-$, respectively (see Figure 1). For $v \in \mathcal{V}$ we define $v^{+/-} := v|_{\partial K^{+/-}}$ and set

$$\{v\} = \frac{1}{2}\left(v^+ + v^-\right), \qquad [\![v]\!] = v^+\mathbf{n}^+ + v^-\mathbf{n}^- \quad \text{on } E \in \mathcal{E}_0.$$

For a piece-wise smooth vector-valued function $\mathbf{q} \in \mathcal{Q}$ the definitions are similar and we set

$$\{\mathbf{q}\} = \frac{1}{2}\left(\mathbf{q}^+ + \mathbf{q}^-\right), \qquad [\![\mathbf{q}]\!] = \mathbf{q}^+ \cdot \mathbf{n}^+ + \mathbf{q}^- \cdot \mathbf{n}^- \quad \text{on } E \in \mathcal{E}_0.$$

On $E \in \mathcal{E}_D \cup \mathcal{E}_N$ the functions $v$ and $\mathbf{q}$ are uniquely defined and we only require $[\![v]\!]$ and $\{\mathbf{q}\}$, which are set as

$$[\![v]\!] = v\mathbf{n}, \qquad \{\mathbf{q}\} = \mathbf{q}.$$

Finally, on $\mathcal{V}$ we define the following weighted broken norm:

$$|\!|\!| v_h |\!|\!|^2 = (A\nabla_h v_h, \nabla_h v_h)_{\mathcal{T}_h} + \alpha h_E^{-1} \langle [\![v_h]\!], [\![v_h]\!]\rangle_{\mathcal{E}_0\cup\mathcal{E}_D}. \tag{2.4}$$

Let us now recall DG formulation for second order elliptic problems. In last several years a large number of DG FEM were developed (see, e.g. [3, 12] and the references therein) for elliptic boundary value problems. Below, we consider the standard interior penalty (IP) DG method, see, e.g., [2, 3]. For the problem (2.1), the primal IP-DG formulation can be stated as follows:
Find $u_h \in \mathcal{V}$ such that

$$\mathcal{A}(u_h, v) = \mathcal{L}(v), \quad \forall v \in \mathcal{V}, \tag{2.5}$$

where the bilinear form $\mathcal{A}(\cdot,\cdot) : \mathcal{V} \times \mathcal{V} \to \mathbb{R}$ and the linear form $\mathcal{L}(\cdot) : \mathcal{V} \to \mathbb{R}$ are defined by the relations

$$\begin{aligned}\mathcal{A}(u_h, v) =& (A\nabla_h u_h, \nabla_h v)_{\mathcal{T}_h} + \alpha h_E^{-1} \langle [\![u_h]\!], [\![v]\!]\rangle_{\mathcal{E}_0\cup\mathcal{E}_D} \\ &- \langle \{A\nabla_h u_h\}, [\![v]\!]\rangle_{\mathcal{E}_0\cup\mathcal{E}_D} - \langle [\![u_h]\!], \{A\nabla_h v\}\rangle_{\mathcal{E}_0\cup\mathcal{E}_D},\end{aligned} \tag{2.6a}$$

$$\mathcal{L}(v) = \int_\Omega f v dx + \alpha h_E^{-1} \langle u_0, v\rangle_{\mathcal{E}_D} - \langle u_0\mathbf{n}, A\nabla_h v\rangle_{\mathcal{E}_D} + \langle g_N, v\rangle_{\mathcal{E}_N}. \tag{2.6b}$$

Here $\alpha$ is a parameter which is to be defined to guarantee the coercivity of the bilinear form $\mathcal{A}$.

As usual, we assume that the Dirichlet boundary condition are defined by a given function $u_0 \in H^1(\Omega)$ in the sense that the trace of $u - u_0$ on $\Gamma_D$ is zero. For the sake of simplicity, we also assume that $u_0$ is such that the boundary condition can be exactly satisfied by the approximations used.

It can be proved (see, e.g., [2, 3]) that the bilinear form $\mathcal{A}$ is coercive and bounded on $\mathcal{V}$ equipped with the norm (2.4) provided that $\alpha > 0$ is sufficiently large. Recently, a lower bound and explicit expression for $\alpha$ to guarantee the coercivity was obtained in [36]. Moreover, it is well known that for $f \in L^2(\Omega)$ the problem (2.5) is well-posed and possesses a unique solution $u_h \in \mathcal{V}$. Assume that $u \in H^s(\Omega)$, $2 \leqslant s \leqslant r+1$. Then, an optimal order of convergence, given by the following estimates, can be obtained in both the norms $|||\cdot|||$ and $\|\cdot\|$

$$|||u - u_h||| \leqslant Ch^{s-1} \|u\|_{H^s(\Omega)},$$
$$\|u - u_h\|_{L^2(\Omega)} \leqslant Ch^s \|u\|_{H^s(\Omega)}.$$

For the proof we refer to [3, 23].

## 3. Functional a posteriori estimates for conforming approximations

Functional type a posteriori error estimates for conforming approximations of a wide spectrum of problems have been derived in [30, 31, 32, 34], see [29] for an overview. In this Section, to keep this article as self content as possible, we briefly recall some principal facts of this error estimation theory.

Let $\tilde{u}_h \in \mathcal{V}_0 + u_0$ be a certain conforming approximation of the exact solution $u$ of the problem (2.1). Then, the following estimate holds ([30]-[32]):

$$\|\nabla(u - \tilde{u}_h)\|_a^2 \leqslant (1+\beta) D(\nabla\tilde{u}_h, y) + \left(1 + \frac{1}{\beta}\right) C_{\Omega,A}^2 \|\mathrm{div} y + f\|^2, \tag{3.1}$$

where

$$\begin{aligned} D(\nabla\tilde{u}_h, y) &= \int_\Omega (A\nabla\tilde{u}_h \cdot \nabla\tilde{u}_h + A^{-1}y \cdot y - 2\nabla\tilde{u}_h \cdot y)dx \\ &= \int_\Omega (A\nabla\tilde{u}_h - y) \cdot (\nabla\tilde{u}_h - A^{-1}y)dx. \end{aligned}$$

In (3.1) $y$ is a "free" vector-valued function in $H(\Omega, \mathrm{div})$, $\beta > 0$, and $C_{\Omega,A}$ is a constant in the inequality

$$\|\underline{v}\| \leqslant C_{\Omega,A} \|\nabla\underline{v}\|_a, \quad \forall \underline{v} \in \mathcal{V}_0. \tag{3.2}$$

If $\Omega \subset \Omega_\square$, where $\Omega_\square$ is a square domain with the side $l$, then $C_{\Omega,A} \leqslant c_2 \frac{l}{\sqrt{d\pi}}$. The constant $c_2$ in this estimate comes from (2.2).

It is easy to see that (3.1) can also be presented in the form

$$\|\nabla(u - \tilde{u}_h)\|_a \leqslant \|A\nabla\tilde{u}_h - y\|_{\bar{a}} + C_{\Omega,A} \|\mathrm{div} y + f\|. \tag{3.3}$$

For $y = A\nabla u$ the right hand side of (3.3) coincides with the left hand one. Thus, the upper bound is sharp in the sense that for any $\tilde{u}_h$ there is a sequence of $y_k$ such that the upper bound computed with help of these functions is as close to the exact error norm as it is desired.

Lower bound of the approximation error is given by the estimate (see, e.g., [33])

$$\|\nabla(u - \tilde{u}_h)\|_a^2 \geqslant -\|\nabla w\|_a^2 - 2\int_\Omega A\nabla\tilde{u}_h \cdot \nabla w dx + 2\int_\Omega f w dx. \tag{3.4}$$

Here $w$ is a "free" function in $\mathcal{V}_0$ which should be selected in such a way that the value of the right hand side be maximal. For $w = u - \tilde{u}_h$ we have from (2.3)

$$-\int_\Omega A\nabla\tilde{u}_h \cdot \nabla w dx + \int_\Omega f w dx = \|\nabla(u - \tilde{u}_h)\|_a^2.$$

Therefore, for $w = u - \tilde{u}_h$ the right hand side of the estimate (3.4) coincides with the left hand one. Thus, the lower bound also has no "gap" and by a proper choice of $w$ we can always make this bound as sharp as it is required.

Summarizing, we say that for *any conforming approximation* $\tilde{u}_h$ two-sided computable bounds of the error can be obtained in the form

$$M_\ominus(w, \tilde{u}_h) \leqslant \|\nabla(u - \tilde{u}_h)\|_a^2 \leqslant M_\oplus(\tilde{u}_h, y, \beta, C_{\Omega,A}), \tag{3.5}$$

where $M_\ominus$ and $M_\oplus$ are the minorant and majorant defined by the right hand side of (3.4) and (3.1), respectively. Computable bounds are obtained if we substitute in (3.5) certain $w$ and $y$ defined on the basis of computed solutions or maximize (minimize) the bounds with respect to some finite dimensional subspaces $\mathcal{V}_\tau$ and $Y_\sigma$.

**Remark 3.1.** *The estimate (3.3) is valid when $\Gamma_D = \partial\Omega$. In the presence of Neumann boundary condition, it has the form*

$$\|\nabla(u - \tilde{u}_h)\|_a \leqslant \|A\nabla\tilde{u}_h - y\|_{\bar{a}} + C_{\Omega,A}\|\mathrm{div} y + f\| + C_{\Gamma,A}\|y\cdot\mathbf{n} - g_N\|_{\Gamma_N}, \tag{3.6}$$

*where $C_{\Gamma,A}$ is a constant in the inequality (similar to that of (3.2))*

$$\|\underline{v}\|_{\Gamma_N} \leqslant C_{\Gamma,A}\|\nabla\underline{v}\|_a, \quad \forall \underline{v} \in \mathcal{V}_0. \tag{3.7}$$

## 4. Functional a posteriori estimates for DG approximations

In this Section, we derive two-sided a posteriori bounds of the approximation errors for DG solutions. Our analysis is based upon the functional a posteriori estimates briefly recalled in the previous Section. The derivation of estimates is performed in two steps: (1) using a certain post-processing procedure that maps the DG approximation to the energy space of the problem considered, and then (2) applying the functional type a posteriori estimate to this post-processed function.

### 4.1. Upper bound of the approximation error.

Let us obtain an upper bound for the quantity $|\!|\!|u - u_h|\!|\!|$. Note that if $\tilde{u}_h \in H^1$, then the "brocken norm" $|\!|\!|\tilde{u}_h|\!|\!|$ coincides with $\|\nabla\tilde{u}_h\|_a$. Therefore,

$$|\!|\!|u - u_h|\!|\!| \leqslant \|\nabla(u - \tilde{u}_h)\|_a + |\!|\!|u_h - \tilde{u}_h|\!|\!| \qquad \forall v \in \mathcal{V}_0 + u_0. \tag{4.1}$$

Using (3.3) in (4.1) we obtain

$$|\!|\!|u - u_h|\!|\!| \leqslant \|A\nabla\tilde{u}_h - y\|_{\bar{a}} + C_{\Omega,A}\|\mathrm{div} y + f\| + |\!|\!|u_h - \tilde{u}_h|\!|\!|. \tag{4.2}$$

Here $\tilde{u}_h$ and $y$ are "free" functions. Note that if $\tilde{u}_h = u$ and $y = A\nabla u$ then the left and right hand sides of (4.1) coincide. Therefore, this estimate is also sharp and has no "gap". However, to obtain a good upper bound of the error in the broken norm we need to suggest a proper choice (discussed in Section 5) of $\tilde{u}_h$ and $y$. Once such functions have been selected, the right hand sides of (4.2) present a natural decomposition of the overall error into three terms:

- *error due to nonconformity*,
- *error in the duality relation for fluxes*,
- *error in the equilibrium equation for fluxes.*

4.2. **Lower bound of the approximation error.** Lower bound of the error in the broken norm for the quantity $|\!|\!|u - u_h|\!|\!|$ is derived in a similar way. For $\tilde{u}_h \in H^1$ we get

$$|\!|\!|u - u_h|\!|\!| \geqslant \|\nabla(u - \tilde{u}_h)\|_a - |\!|\!|u_h - \tilde{u}_h|\!|\!| \qquad \forall \tilde{u}_h \in \mathcal{V}_0 + u_0. \tag{4.3}$$

Using (3.4) in (4.3) we obtain

$$|\!|\!|u - u_h|\!|\!| \geqslant \left(-\|\nabla w\|_a^2 - 2\int_\Omega A\nabla\tilde{u}_h \cdot \nabla w dx + 2\int_\Omega f w dx\right)^{\frac{1}{2}} - |\!|\!|u_h - \tilde{u}_h|\!|\!|\,. \tag{4.4}$$

In this relation, $w$ is a "free" function. This estimate is also sharp since the left hand side coincides with the right hand side for $w = u - \tilde{u}_h$ and $\tilde{u}_h = u$. A proper choice of $\tilde{u}_h$ and $w$ is discussed in Section 5.

## 5. Computing "free" functions in upper and lower bounds

There are two basic ways to define the "free" functions in a posteriori error estimates. The first (cheap) way is to define them by a certain post-processing of the data contained in the approximate solutions. The second way is related to minimization (maximization) procedures intended to define the upper and lower bounds as close to the exact error as possible.

5.1. **A mapping from $\mathcal{V}$ to $\mathcal{V}_0 + u_0$.** Both upper and lower bounds for the DG approximations contain an additional term $|\!|\!|u_h - \tilde{u}_h|\!|\!|$. It is clear that the function $\tilde{u}_h$ should be taken such that this term be minimal. Below, we present two basic ways to compute $\tilde{u}_h$. Let $\Pi : \mathcal{V} \to \mathcal{V}_\tau \subset \mathcal{V}_0 + u_0$ be a projection operator that maps the space of discontinuous piece-wise polynomial functions to the space of continuous piece-wise polynomial functions (on the partitioning corresponding to $\mathcal{V}_\tau$, see Figure 2). We shall consider the following projections:

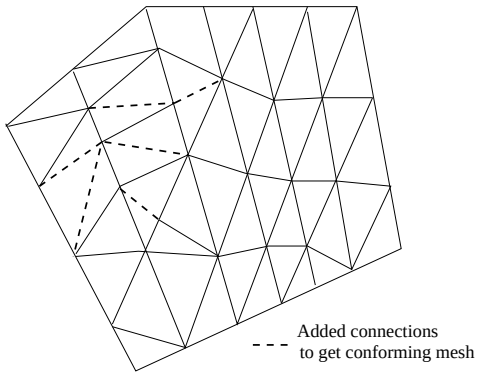


FIGURE 2. A possible DG triangulation: An irregular mesh (continuous lines) completed by adding new elements (dashed line) to make a conforming triangular mesh

(1) Projection obtained by a simple averaging of the values of $u_h$ at the vertices.
(2) The orthogonal projection of $u_h$ on the energy space constructed with respect to a broken norm.

For the sake of consistency of the notations for conforming approximations we shall denote both the projections by $\tilde{u}_h$.

5.1.1. *Projection obtained by a simple averaging.* Assume that DG approximations are constructed such that on each element $K_i \in \mathcal{T}_h$ the approximate solution $u_h$ is a polynomial of the order $r$. Our goal is to construct a *post-processing operator* $\Pi : \mathcal{V} \to \mathcal{V}_\tau \subset \mathcal{V}_0 + u_0$ with the following properties:

- $\Pi u_h$ and $u_h$ are close in $L^2$ norm,
- $\Pi u_h$ is a continuous piece wise affine function that is close or equal to the DG solution $u_h$ except possibly in small regions associated with boundary layers, and
- if DG solution indicates the presence of boundary layers, which are approximated in $u_h$ as interelement jumps, then in the respective parts $\Pi u_h$ has zones with high gradients whose size is automatically defined on the basis on the minimal energy principle.

To construct $\Pi u_h$ we proceed as follows. Consider a patch of elements that has a common node $\mathcal{N}$. If $\mathcal{N}$ is internal, then we set the value of $\Pi u_h$ on it as the mean value of the respective nodal values of the neighboring simplexes (such nodes are marked by big dots in Fig. 3. If the node belongs to the Dirichlet boundary, then the respective value is defined by $u_0$.

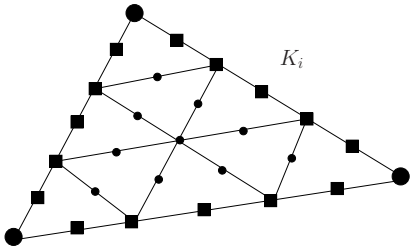


FIGURE 3. Post-processing of $u_h$ on $K_i$

On the edge $E_{ij}$ common for $K_i$ and $K_j$ we define the common value of the trace as a polynomial of the order $r$ that takes the given values at the boundary nodes of the edge. Other $r-1$ values are defined as mean values of $u_h$ on $K_i$ and $K_j$ at $r-1$ points of $E_{ij}$ uniformly distributed between the two end points, see squares on Fig. 3. Now, on each simplex the boundary values are fully defined by means of $u_h$. To extend these values inside the simplexes we apply a certain post-processing procedure on each simplex. First, using baricentrical coordinates, we subdivide a simplex $K_i$ in $m_i$ subelements, see Fig. 3. In the simplest case, such a subdivision can be performed by similar simplexes, but in general, any other regular family of elements can be used. At all boundary nodes the values are defined by the given values of the trace. At all internal nodes $i_s$ (small dots on Fig. 3) we set

$$\Pi u_h(x_{i_s}) = u_h(x_{i_s}). \tag{5.1}$$

Now, on $K_i$ the function $\Pi u_h(x)$ is obtained by the extension of these nodal values on each subelement as the polynomial of the order $r$. For example, on Fig. 3 we show the system of local nodes for the case $r = 2$. Once $m_i$ is defined, the respective function of $K_i$ is directly computed without solving any local problems. The only parameter that affects the form of the post-processed function is the number $m_i$ that regulates the structure of the mesh (if the subelements are similar to $K_i$). If

at the neighborhood of $K_i$ the true solution and its approximation $u_h$ are regular and have no big gradients, then the value of $m_i$ will probably play no essential role in the quality of the post-processed function. However, if, e.g., one edge of $K_i$ goes along a boundary layer, so that $u$ has big normal derivatives at the points of the edge and $u_h$ has a jump, then the value of $m_i$ may be essential because it regulates the size of the boundary layer in the post-processed function $\Pi u_h$. Since the latter is a-priori unknown, we should offer some criteria to properly choose $m_i$. For this purpose we suggest the following approach:

Let $\Pi_{K_i}^{m_i}$ defines the above described local post-processing operator on $K_i$. Define $m_i^*$ such that

$$J_{K_i}(\Pi_{K_i}^{m_i^*} u_h) \leqslant J_{K_i}(\Pi_{K_i}^{m_i} u_h) \quad \forall m_i = 2, 3, ..., \tag{5.2}$$

where $J$ is the local energy functional

$$J_{K_i}(v) := \int_{K_i} (A\nabla v \cdot \nabla v - fv)\, dx. \tag{5.3}$$

We recall that the problem (2.3) has a variational formulation

$$\inf_{v \in \mathcal{V}_0 + u_0} J(v),$$

where

$$J(v) = \frac{1}{2} a(v, v) - \int_\Omega fv dx.$$

Thus, the structure of the local functional used to determine $m_i^*$ is dictated by the global energy functional. In other words, we select the size of the boundary layer that may appear after post-processing of the DG solution and is defined automatically with the help of the *energy principle* that comes from the variational formulation of the problem considered. It is worth outlining that in the construction of our post-processing operator $\Pi$ no local boundary value problems are solved. For each particular natural number $m_i^*$, it is only required to find $J_{K_i}(\Pi_{K_i}^{m_i} u_h)$, which is the sum of integrals on subelements of $K_i$ computed by (5.3). Since all the nodal values are explicitly defined, this procedure is computationally inexpensive.

We have discussed the case, in which $\Omega$ is divided into a collection of simplexes. However, the post-processing procedure discussed is easily extended to other types of elements (e.g., quadrilateral) in 2D as well as in 3D.

This is a cheaper way of mapping onto the space $\mathcal{V}_0 + u_0$, which may be viewed as a certain post-processing operator. However, if more accurate results are desired we suggest the following orthogonal projection on the broken energy space.

5.1.2. *The orthogonal projection on the energy space.* In this approach we set $\Pi u_h = \tilde{u}_h$, where

$$\left\| \left[ u_h - \tilde{u}_h \right] \right\| = \inf_{\underline{u_h} \in \mathcal{V}_\tau} \left\| \left[ u_h - \underline{u_h} \right] \right\|. \tag{5.4}$$

In other words, this is the DG-projection defined as follows: Find $\tilde{u}_h \in \mathcal{V}_\tau$ such that $\mathcal{A}(\tilde{u}_h, v) = \mathcal{A}(u_h, v)$ for all $v \in \mathcal{V}_\tau$. Here $\mathcal{A}(\cdot, \cdot)$ is the bilinear form of the DG method, defined in (2.6a). We outline that in (5.4) the space $\mathcal{V}_\tau$ is not necessarily the same as $\mathcal{V}$ used in the DG method and may be constructed on the mesh which does not coincide with the mesh $\mathcal{T}_h$ used in the DG method.

If $u$ is sufficiently regular and $u_h \to u$, then the above terms are small. Let $I_\tau$ be the standard interpolation operator on the mesh $\mathcal{T}_\tau$. Now, since

$$|||u_h - \tilde{u}_h||| \leqslant |||u_h - I_\tau u|||,$$

we observe that

$$\begin{aligned} |||u_h - \tilde{u}_h||| &\leqslant |||u_h - u||| + |||u - I_\tau u||| \\ &= |||u_h - u||| + \|\nabla(u - I_\tau u)\|_a. \end{aligned} \tag{5.5}$$

Under the usual assumptions that provide qualified convergence of DG approximations and the respective interpolation estimates in the conforming space we find that the right-hand side of (5.5) is of the order $h^r + \tau^r$, where $r$ denotes the approximating polynomial order.

It is important to note, however, that if the DG method is used to obtain in a sense good approximation of a solution with high gradients, boundary layers, etc. on a coarse mesh, then orthogonal projection on $\mathcal{T}_h$ may be ineffective because continuous approximations on such a mesh are unable to present the shape of the true solution. In this case, it is desirable that $\mathcal{V}_\tau$ be constructed on a much finer mesh $\mathcal{T}_\tau$. However, finding the exact orthogonal projection of $u_h$ on a certain (finer) subspace $\mathcal{V}_\tau$ may present a task whose cost is comparable with the cost required for finding $u_h$ on a coarse mesh $\mathcal{T}_h$. This could lead to extra computational expenditures in the above *modus operandi*. Also, one encounters difficulties if hanging nodes are present in the coarse mesh on which the DG solution is computed.

5.2. **Recovering of the flux $y$.** In practice, we have three basic ways to define a suitable flux $y$. The first is to use the approximate solution computed and recover the flux by some post–processing procedure. Minimization of the Majorant on a certain finite dimensional subspace of $H(\Omega, \mathrm{div})$ gives another way. The third group of methods is based on the attraction of DG formulations to compute the desired flux.

5.2.1. *Post-processing on the primal mesh.* We can use an approximate solution $\tilde{u}_h$ to compute an approximation of the flux $y_h := A\nabla_h u_h \in L^2(\Omega, \mathbb{R}^d)$ and find a vector-valued function $\tilde{y}_h \in H(\Omega, \mathrm{div})$ (which is close to $y_h$ in $L^2$-sense) by a certain post-processing (averaging) operator $G_h : L^2(\Omega, \mathbb{R}^d) \to H(\Omega, \mathrm{div})$. Such an operator can be constructed in a way similar to that was used above for the function $\tilde{u}_h$. On each edge common to two simplexes we define the normal component of $\tilde{y}_h$ as the mean value of the two neighbor sides and further extend it inside each element by means of auxiliary subelement subdivision. In this case, it is natural to use Raviart-Thomas elements of the respective order and define the normal fluxes on edges inside $K_i$ by means of $y_h$ and on the edges of $K_i$ from the averaged values defined above. The size of the boundary layer and the number $m_i^*$ comes from the respective post-processing procedure for $u_h$. The latter procedure gives a *directly computable estimate*

$$\begin{aligned} |||u - u_h||| \leqslant &\left( \int_\Omega (A\nabla\tilde{u}_h - \tilde{y}_h) \cdot (\nabla\tilde{u}_h - A^{-1}\tilde{y}_h) dx \right)^{\frac{1}{2}} \\ &+ C_{\Omega,A} \|\mathrm{div}\tilde{y}_h + f\| + |||u_h - \tilde{u}_h|||. \end{aligned} \tag{5.6}$$

This method is cheap, but the respective upper bound may be rather coarse.

5.2.2. *Post-processing on the refined mesh.* Better estimates can be obtained if a problem is solved on a sequence of refined meshes $\mathcal{T}_1, \mathcal{T}_2, \ldots, \mathcal{T}_{k-1}, \mathcal{T}_k = \mathcal{T}_\tau$. For the sake of simplicity we denote $u_i := u_{h_i}$, where $i$ denotes the refinement level. Now let $\tilde{u}_1, \tilde{u}_2, \ldots, \tilde{u}_k$ be a sequence of the respective approximate solutions. Compute $y_\tau := A\nabla_h u_k$ and use an averaging operator $G_k$ on $\mathcal{T}_k$ to construct a "regularized" flux $\tilde{y}_\tau$. Then, for $u_{k-1}$ we have the estimate

$$\begin{aligned} |||u - u_{k-1}||| \leqslant &\left(\int_\Omega (A\nabla\tilde{u}_{k-1} - \tilde{y}_\tau)\cdot(\nabla\tilde{u}_{k-1} - A^{-1}\tilde{y}_\tau)dx\right)^{\frac{1}{2}} \\ &+ C_{\Omega,A}\,\|\mathrm{div}\tilde{y}_\tau + f\| + |||u_h - \tilde{u}_{k-1}|||\,. \end{aligned} \tag{5.7}$$

This estimate is also computationally inexpensive. Since the image of the flux computed on a refined mesh is more accurate, this estimate is, in general, much sharper than (5.6).

**Remark 5.1.** *This estimate can be viewed as a quantitative form of the Runge's rule for DG approximations.*

5.2.3. *Minimization of the Majorant.* If we need to have a sharp upper bound of the approximation error on a particular mesh $\mathcal{T}_h$, then it is better to apply a method different from the above described. In this method, we select a finite dimensional subspace $\mathcal{Y} \subset H(\Omega, \mathrm{div})$ and minimize the Majorant on $\mathcal{Y}$. In other words, we use the estimate

$$\begin{aligned} |||u - u_h||| \leqslant \Big(\inf_\beta \inf_{\tilde{y}_h\in\mathcal{Y}} \Big\{(1+\beta)\int_\Omega (A\nabla\tilde{u}_h - \tilde{y}_h)\cdot(\nabla\tilde{u}_h - A^{-1}\tilde{y}_h)dx \\ +(1+1/\beta)C^2_{\Omega,A}\,\|\mathrm{div}\tilde{y}_h + f\|^2\Big\}\Big)^{\frac{1}{2}} + |||u_h - \tilde{u}_h|||\,. \end{aligned} \tag{5.8}$$

The wider $\mathcal{Y} \subset H(\Omega, \mathrm{div})$ we take the sharper upper bound we obtain. For any $\beta > 0$, the right hand side of the estimate is a quadratic functional, whose minimization can be performed by standard numerical procedures. In practice, it is convenient to minimize the functional with respect to one of the variables $\beta$ or $y$ while keeping the other fixed. Though minimization with respect to $\beta$ requires only evaluation of integrals, however, minimization with respect to $y$ requires solving a system of equations for a vector-valued function. Overall, this interleaved process requires few steps, and hence, computationally this approach is not cheap.

5.2.4. *Averaging of the flux obtained by the DG formulation.* In this method, we compute $y_h$ from the DG formulation. We know that the primal formulation of the IP-DG method (2.5) can also be derived from a mixed formulation involving an auxiliary variable $y_h = A\nabla_h u_h$, for details see [3]. This gives $y_h$ by solving the following equation element-wise $\forall q \in \mathcal{Q}$

$$\begin{aligned} \int_K y_h\cdot q dx = \int_K A\nabla_h u_h\cdot q dx - \sum_{E\in\partial K\cap(\Gamma_0\cup\Gamma_D)}\int [\![u_h]\!]\cdot\{q\}\,ds \\ + \sum_{E\in\partial K\cap\Gamma_D}\int u_0\mathbf{n}\cdot q ds. \end{aligned} \tag{5.9}$$

We then use some averaging operator $G_h$ to construct a "regularized" flux $\tilde{y}_h$. This method can be considered as an alternative to the method presented in Section 5.2.1, however, its performance would not differ much.

5.3. **Computation of lower error bounds.** Let us briefly discuss the practical implementation of the estimate (3.4). The function $w$ can be defined in the same way as $y$ in the Majorant. For example, if we use a sequence of refined meshes $\mathcal{T}_1, \mathcal{T}_2, \dots, \mathcal{T}_k$ and compute the respective $u_1, u_2, \dots, u_k$, then a cheap way to compute lower bounds consists of setting $w = \tilde{u}_k - \tilde{u}_{k-1}$. In this case, (3.4) implies the estimate

$$\begin{aligned} |||u - u_{k-1}||| \geqslant & \left( -\|\nabla w\|_a^2 + 2\int_\Omega f w dx - 2\int_\Omega A\nabla \tilde{u}_{k-1} \cdot \nabla w dx \right)^{\frac{1}{2}} \\ & - |||u_h - \tilde{u}_{k-1}||| . \end{aligned} \tag{5.10}$$

If a more accurate lower bound is required, then it is necessary to maximize the minorant (the functional in the right hand side of (3.4)) on a certain subspace $\mathcal{V}_0$ which is bigger than $\mathcal{V}$. One way to create such a subspace is to add additional trial functions (e.g., "bubble functions") to $\mathcal{V}$. In this case,

$$\begin{aligned} |||u - u_h||| \geqslant & \Big( \sup_{w \in \mathcal{V}_0} \Big\{ -\|\nabla w\|_a^2 - 2\int_\Omega A\nabla \tilde{u}_h \cdot \nabla w dx + 2\int_\Omega f w dx \Big\} \Big)^{\frac{1}{2}} \\ & - |||u_h - \tilde{u}_h||| . \end{aligned} \tag{5.11}$$

**Remark 5.2.** *Note that the estimates derived for bounds of the approximation errors and the methods suggested to compute the "free" functions still hold if instead of (2.4) one chooses the discrete energy norm defined as* $|||v|||^2 := (A\nabla v, \nabla v)_{\mathcal{T}_h}$.

## 6. Numerical results

In this Section we present numerical examples which aim to verify the theoretical results and confirm the efficiency of the proposed technique to compute the upper-bounds of the approximation error. For brevity reasons we consider the computation of $\tilde{u}_h$ only by the orthogonal projection (Section 5.1.2) and the computation of $y$ only by the minimization of the majorant (Section 5.2.3).

We define the majorant for the DG solution as the right hand side of (5.8) and denote it by $M_\oplus^{\mathrm{DG}}$. The effectivity Ieff of the majorant is then computed as

$$\mathrm{Ieff} = M_\oplus^{\mathrm{DG}} / |||u - u_h||| .$$

For simplicity we assume $A$ in (2.1) to be an identity matrix. We first consider the following 1-D examples.

**Example 6.1.** *Consider the Poisson problem on a unit interval*

$$\begin{aligned} -u'' &= f, \qquad \text{in } \Omega \equiv (0,1) , \\ u &= 0, \qquad \text{at } \partial\Omega. \end{aligned}$$

*Choose $f$ such that the analytic solution of the problem is $u = x(1-x)$.*

**Example 6.2.** *Consider the domain and equations of example 6.1. Now choose $f$ such that the analytic solution of the problem is $u = x(1-x)\exp(2x)$.*

We use linear polynomials to approximate all the desired quantities, i.e. the DG solution $u_h$, its projection on a conforming space $\tilde{u}_h$, and the vector-valued function $y$ required to compute the majorant. Various errors for these numerical examples, which satisfy the inequality (4.1), are presented in Tables 1, and 3, respectively. The error induced by the projection of DG solution onto conforming space is quite small as compared to the errors between analytic solution and the DG solution or between

TABLE 1. Various errors for numerical example 6.1

| DOF | $\|\|\|\tilde{u}_h - u_h\|\|\|$ I | $\|\nabla(u - \tilde{u}_h)\|_a$ II | I+II | $\|\|\|u - u_h\|\|\|$ |
|---|---|---|---|---|
| 20 | 1.272e-03 | 5.779e-02 | 5.906e-02 | 5.775e-02 |
| 40 | 4.519e-04 | 2.888e-02 | 2.933e-02 | 2.887e-02 |
| 80 | 1.608e-04 | 1.444e-02 | 1.460e-02 | 1.443e-02 |
| 160 | 5.748e-05 | 7.218e-03 | 7.275e-03 | 7.217e-03 |
| 320 | 2.074e-05 | 3.609e-03 | 3.629e-03 | 3.608e-03 |

TABLE 2. Effectivity of the majorant for numerical example 6.1

| DOF | $\beta$ | $\|\|\|\tilde{u}_h - u_h\|\|\|^2$ | $\|\nabla\tilde{u}_h - y\|_a^2$ | $\|\nabla \cdot y + f\|^2$ | Ieff |
|---|---|---|---|---|---|
| 20 | 0.001 | 1.617e-06 | 3.339e-03 | 2.690e-08 | 1.023 |
| 40 | 0.000 | 2.042e-07 | 8.341e-04 | 1.234e-10 | 1.016 |
| 80 | 0.000 | 2.586e-08 | 2.084e-04 | 5.241e-13 | 1.011 |
| 160 | 0.000 | 3.304e-09 | 5.209e-05 | 2.137e-15 | 1.008 |
| 320 | 0.000 | 4.302e-10 | 1.302e-05 | 8.526e-18 | 1.006 |

TABLE 3. Various errors for numerical example 6.2

| DOF | $\|\|\|\tilde{u}_h - u_h\|\|\|$ I | $\|\nabla(u - \tilde{u}_h)\|_a$ II | I+II | $\|\|\|u - u_h\|\|\|$ |
|---|---|---|---|---|
| 20 | 2.215e-02 | 4.274e-01 | 4.496e-01 | 4.268e-01 |
| 40 | 8.577e-03 | 2.155e-01 | 2.241e-01 | 2.153e-01 |
| 80 | 3.178e-03 | 1.079e-01 | 1.111e-01 | 1.079e-01 |
| 160 | 1.155e-03 | 5.397e-02 | 5.513e-02 | 5.396e-02 |
| 320 | 4.179e-04 | 2.698e-02 | 2.740e-02 | 2.698e-02 |

TABLE 4. Effectivity of the majorant for numerical example 6.2

| DOF | $\beta$ | $\|\|\|\tilde{u}_h - u_h\|\|\|^2$ | $\|\nabla\tilde{u}_h - y\|_a^2$ | $\|\nabla \cdot y + f\|^2$ | Ieff |
|---|---|---|---|---|---|
| 20 | 0.168 | 4.908e-04 | 1.802e-01 | 5.010e-02 | 1.213 |
| 40 | 0.086 | 7.357e-05 | 4.625e-02 | 3.374e-03 | 1.125 |
| 80 | 0.044 | 1.010e-05 | 1.163e-02 | 2.208e-04 | 1.073 |
| 160 | 0.022 | 1.335e-06 | 2.912e-03 | 1.415e-05 | 1.044 |
| 320 | 0.011 | 1.746e-07 | 7.281e-04 | 8.965e-07 | 1.027 |

analytic solution and the projected solution. Individual terms of the majorant, the constant $\beta$ and the effectivity index for these numerical examples, which satisfy the inequality (4.2), are presented in Tables 2, and 4, respectively. For the example 6.1 since $f$ is a constant function, the term $\|\nabla \cdot y + f\|$, where $y$ is approximated using linear polynomials (and hence, $\nabla \cdot y$ is a constant), is very small. This results in a very good effectivity index. However, for the example 6.2 the function $f$ has steep gradients and hence, can not be accurately approximated by linear polynomials for $y$. In these cases we add a bubble function for the approximation of $y$. The height of these bubble functions are chosen by element-wise minimization of energy

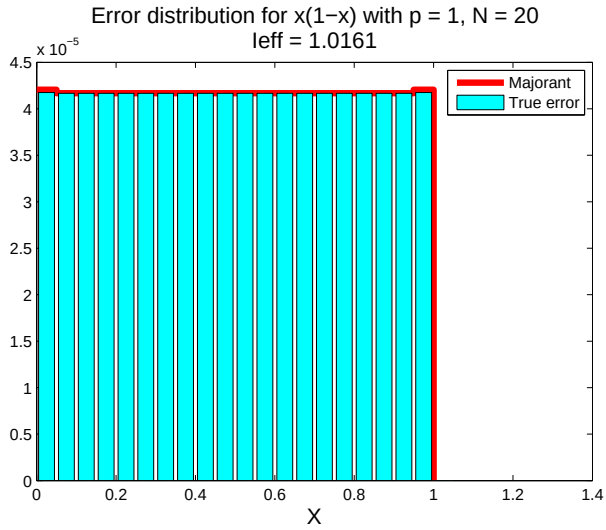


FIGURE 4. For numerical example 6.1 elementwise true error and majorant, $p = 1$ and DOF $= 40$

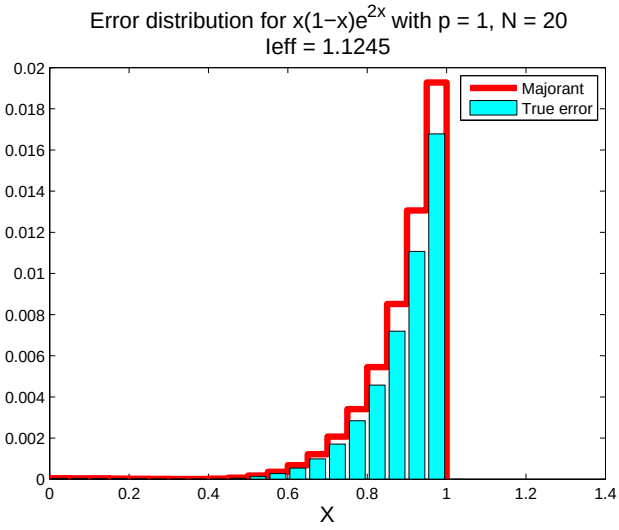


FIGURE 5. For numerical example 6.2 elementwise true error and majorant, $p = 1$ and DOF $= 40$

and hence, this process is computationally inexpensive. Element-wise errors and majorant are depicted in Figures 4, and 5, respectively.

We now present the numerical results for the following 2-D examples:

**Example 6.3.** *Consider the Poisson problem on a unit square*

$$\begin{aligned} -\Delta u &= f, \qquad \text{in } \Omega \equiv (0,1) \times (0,1), \\ u &= 0, \qquad \text{at } \partial\Omega. \end{aligned}$$

*Choose $f$ such that the analytic solution of the problem is $u = sin(2\pi x) sin(2\pi y)$.*

**Example 6.4.** *Consider the domain and equations of example 6.3. Now choose $f$ such that the analytic solution of the problem is $u = x(1-x)y(1-y)\exp(2x+2y)$.*

TABLE 5. Various errors for numerical example 6.3

| DOF | $\|\!\|\!\|\tilde{u}_h - u_h\|\!\|\!\|$ I | $\|\nabla(u-\tilde{u}_h)\|_a$ II | I+II | $\|\!\|\!\|u - u_h\|\!\|\!\|$ |
|---|---|---|---|---|
| 900 | 4.092e-03 | 6.526e-02 | 6.936e-02 | 6.537e-02 |
| 3600 | 7.874e-04 | 1.634e-02 | 1.712e-02 | 1.635e-02 |
| 14400 | 1.437e-04 | 4.085e-03 | 4.229e-03 | 4.088e-03 |
| 57600 | 2.575e-05 | 1.021e-03 | 1.047e-03 | 1.022e-03 |

TABLE 6. Effectivity of the majorant for numerical example 6.3

| DOF | $\beta$ | $\|\!\|\!\|\tilde{u}_h - u_h\|\!\|\!\|^2$ | $\|\nabla\tilde{u}_h - y\|_a^2$ | $\|\nabla \cdot y + f\|^2$ | Ieff |
|---|---|---|---|---|---|
| 900 | 0.226 | 1.674e-05 | 7.338e-03 | 7.401e-03 | 1.669 |
| 3600 | 0.190 | 6.200e-07 | 4.563e-04 | 3.245e-04 | 1.602 |
| 14400 | 0.181 | 2.066e-08 | 2.841e-05 | 1.834e-05 | 1.575 |
| 57600 | 0.179 | 6.633e-10 | 1.773e-06 | 1.117e-06 | 1.561 |

TABLE 7. Various errors for numerical example 6.4

| DOF | $\|\!\|\!\|\tilde{u}_h - u_h\|\!\|\!\|$ I | $\|\nabla(u-\tilde{u}_h)\|_a$ II | I+II | $\|\!\|\!\|u - u_h\|\!\|\!\|$ |
|---|---|---|---|---|
| 900 | 1.229e-03 | 1.989e-02 | 2.112e-02 | 1.993e-02 |
| 3600 | 2.356e-04 | 5.000e-03 | 5.235e-03 | 5.005e-03 |
| 14400 | 4.337e-05 | 1.252e-03 | 1.295e-03 | 1.252e-03 |
| 57600 | 7.825e-06 | 3.130e-04 | 3.208e-04 | 3.131e-04 |

TABLE 8. Effectivity of the majorant for numerical example 6.4

| DOF | $\beta$ | $\|\!\|\!\|\tilde{u}_h - u_h\|\!\|\!\|^2$ | $\|\nabla\tilde{u}_h - y\|_a^2$ | $\|\nabla \cdot y + f\|^2$ | Ieff |
|---|---|---|---|---|---|
| 900 | 0.325 | 1.511e-06 | 5.202e-04 | 1.088e-03 | 1.579 |
| 3600 | 0.320 | 5.550e-08 | 3.293e-05 | 6.654e-05 | 1.560 |
| 14400 | 0.318 | 1.881e-09 | 2.065e-06 | 4.133e-06 | 1.548 |
| 57600 | 0.318 | 6.123e-11 | 1.292e-07 | 2.579e-07 | 1.538 |

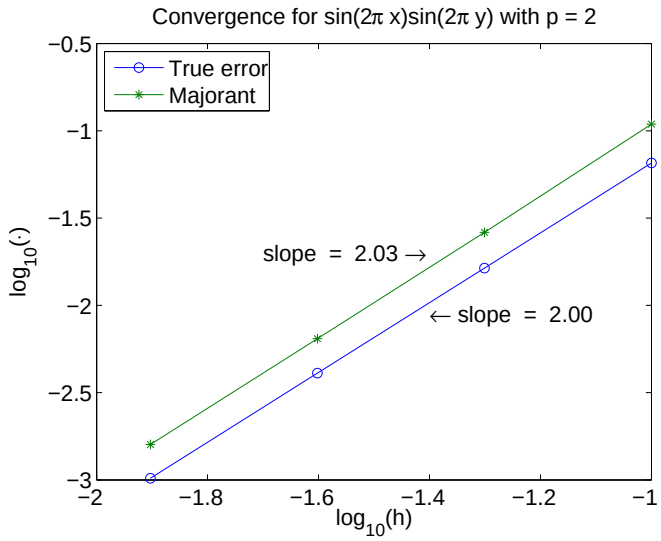


FIGURE 6. For numerical example 6.3 convergence of true error and majorant, $p = 2$

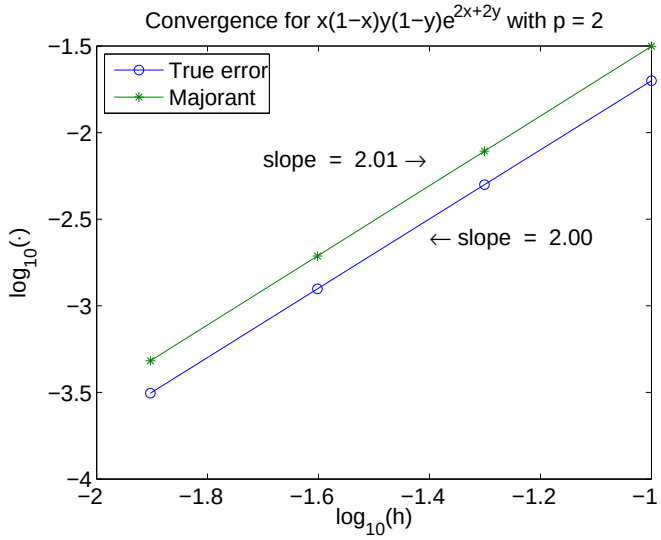


FIGURE 7. For numerical example 6.4 convergence of true error and majorant, $p = 2$

As it is evident from 1-D examples that for problems where $f$ has steep gradients higher order approximations are required for $y$. Hence, for simplicity, instead of devising bubble functions we use quadratic polynomials to approximate all the desired quantities, i.e. the DG solution $u_h$, its projection on a conforming space $\tilde{u}_h$, and $y$. Various errors for these numerical examples, which satisfy the inequality (4.1), are presented in Tables 5 and 7, respectively. The error induced by the projection

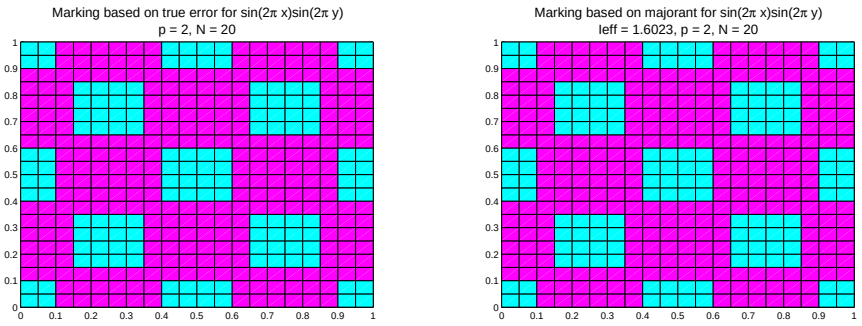


(a) (b)

FIGURE 8. For numerical example 6.3 elements marked for refinement based on true error and majorant, $p = 2$ and DOF $= 3600$

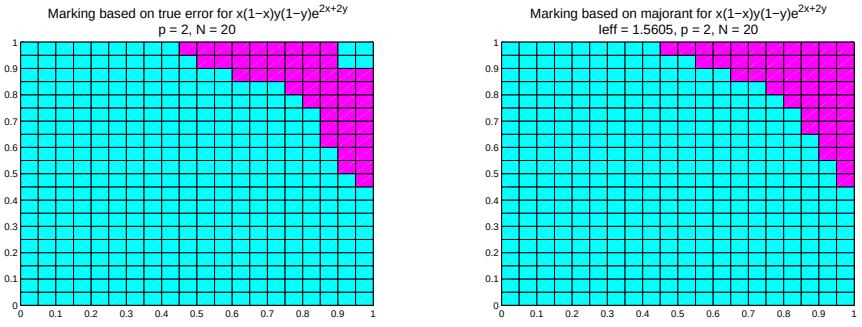


(a) (b)

FIGURE 9. For numerical example 6.4 elements marked for refinement based on true error and majorant, $p = 2$ and DOF $= 3600$

of DG solution onto conforming space is again small as compared to the errors between analytic solution and the DG solution or between analytic solution and the projected solution. Individual terms of the majorant, the constant $\beta$ and the effectivity index for these numerical examples, which satisfy the inequality (4.2), are presented in Tables 6 and 8, respectively. Convergence rates of the DG approximations in the broken energy norm $|||\cdot|||$ and the majorant are shown in Figures 6 and 7 for examples 6.3 and 6.4, respectively. The slopes are computed by fitting a straight line to the given data points in a least-squares sense. Figures 8(a) and 8(b) show the elements marked for refinement (with pink color) based on true error and the majorant, respectively, for the example 6.3. Figures 9(a) and 9(b) show the elements marked for refinement (with pink color) based on true error and the majorant, respectively, for the example 6.4. The refinement criteria is chosen as follows [8, 14]:

Let $\varepsilon_K$ denote the error for the element $K$ in the tessellation $\mathcal{T}_h$. The *max-refinement rule* marks a subset $\mathcal{M}$ of $\mathcal{T}_h$ for refinement according to the following criteria

$$L \in \mathcal{M} \text{ if and only if } \varepsilon_L \geqslant \Theta \max_K \varepsilon_K, \qquad 0 \leqslant \Theta \leqslant 1. \tag{6.1}$$

More efficient refinement criteria, known as *bulk-refinement*, proposed by Dörfler [18] can also be used.

Finally, in table 9 we present the computing time for various parts of the total optimization approach, i.e. time required for the DG solution, its projection onto conforming space, and the majorant computation, for the example 6.3.

TABLE 9. Computing time (sec) for numerical example 6.3

| DOF | DG solution | Projection | Majorant |
|---|---|---|---|
| 900 | 0.900 | 0.056 | 0.499 |
| 3600 | 2.469 | 0.223 | 1.947 |
| 14400 | 9.098 | 0.928 | 8.120 |
| 57600 | 41.898 | 4.0414 | 35.642 |

## ACKNOWLEDGMENTS

This work was initiated during the Special Radon Semester on Computational Mechanics, held at RICAM, Linz, Oct. 3rd - Dec. 16th 2005, and has been conducted in its follow-up phase. The authors gratefully acknowledge the support by the Austrian Academy of Sciences. Authors also thank Professor Ern (CERMICS, ENPC, France) for the suggestion to use DG approximations as a source for a suitable function $y$ in the error majorant.

## REFERENCES

[1] M. Ainsworth and J.T. Oden, *A posteriori error estimation in finite element analysis*, Wiley and Sons, New York, 2000.
[2] D. Arnold, An interior penalty finite element method with discontinuous elements, *SIAM J. Numer. Anal.*, 19 (1982), 742–760.
[3] D. Arnold, F. Brezzi, B. Cockburn and L.D. Marini, Unified analysis of discontinuous Galerkin methods for elliptic problems, *SIAM J. Numer. Anal.*, 39 (2002), 1749–1779.
[4] I. Babuška, The finite element method with penalty, *Math. Comp.*, 27, 122, (1973), 221–228.
[5] I. Babuška and M. Zlamal, Nonconforming elements in the finite element method with penalty, *SIAM J. Numer. Anal.*, 10, 5, (1973), 863–875.
[6] I. Babuška and W.C. Rheinboldt, A posteriori error estimates for the finite element method, *Int. J. Numer. Meth. Engrg.*, 12 (1978), 1597–1615.
[7] I. Babuška and T. Strouboulis, *The finite element method and its reliability*, Clarendon Press, Oxford University Press, New York, 2001.
[8] I. Babuška and M. Vogelius, Feedback and adaptive finite element solution of one-dimensional boundary value problems, *Numer. Math.*, 44 (1984) 75–102.
[9] W. Bangerth and R. Rannacher. *Adaptive finite element methods for differential equations*, Birkhäuser, Berlin, 2003.
[10] R. Becker, P. Hansbo and M.G. Larson, Energy norm a posteriori error estimation for discontinuous Galerkin methods, *Comput. Methods Appl. Mech. Engrg.*, 192 (2003), 723–733.
[11] D. Braess and J. Schöberl, Equilibrated residual error estimator for Maxwell;s equations, Preprint, 2006.

[12] F. Brezzi, B. Cockburn, L.D. Marini and E. Süli, Stabilization mechanisms in discontinuous Galerkin finite element methods, *Report NA-04/24*, Oxford University Computing Laboratory, 2004.
[13] R. Bustinza, G.N. Gatica and B. Cockburn, An a posteriori error estimate for the local discontinuous Galerkin method applied to linear and nonlinear diffusion problems, *Journal of Scientific Computing*, 22-23 (2005), 147–185.
[14] C. Carstensen, A. Orlando and J. Valdman, A convergent adaptive finite element method for the primal problem of elastoplasticity, *Int. J. Numer. Meth. Engrg.*, 67 (2006), 1851–1887.
[15] C. Carstensen and R. Verfürth, Edge residuals dominate a posteriori error estimates for low order finite element methods, *SIAM J. Numer. Anal.*, 36 (1999), 1571–1587.
[16] P. Castillo, An a posteriori error estimate for the local discontinuous Galerkin method, *Journal of Scientific Computing*, 22-23 (2005), 187–204.
[17] Ph. Clément, Approximations by finite element functions using local regularization, *RAIRO Anal. Numér.*, 9 (1975), 77–84.
[18] W. Dörfler, A convergent adaptive algorithm for Poisson's equation, *SIAM J. Numer. Anal.*, 33 (1996) 1106–1124.
[19] A. Ern and J. Proft, A posteriori discontinuous Galerkin error estimates for transient convection-diffusion equations, *Appl. Math. Letters*, 18 (2005) 833–841.
[20] J. Douglas and T. Dupont, *Interior penalty procedures for elliptic and parabolic Galerkin methods*, Lecture Notes in Physics, 58 (1978), 207–216.
[21] P. Houston, R. Rannacher and E. Süli, A posteriori error analysis for stabilized finite element approximations of transport problems, *Comput. Methods Appl. Mech. Engrg.*, 190 (2000), 1483–1508.
[22] C. Johnson and A. Szepessy, Adaptive finite element methods for conservation laws based on a posteriori error estimates, *Commun. Pure and Appl. Math.*, XLVIII (1995), 199–234.
[23] G. Kanschat and R. Rannacher, Local error analysis of the interior penalty discontinuous Galerkin method for second order elliptic problems, *J. Numer. Math.*, 10 (2002), 249–274.
[24] O.A. Karakashian and F. Pascal, A posteriori error estimates for a discontinuous Galerkin approximation of second order elliptic problems, *SIAM J. Numer. Anal.* 41 (2003) 2374–2399.
[25] M. Křížek and P. Neittaanmäki. Superconvergence phenomenon in the finite element method arising from averaging of gradients, *Numer. Math.*, 45 (1984), 105–116.
[26] J. Ma and H. Brunner, A posteriori error estimates of discontinuous Galerkin methods for non-standard Volterra integro-differential equations, *IMA Journal of Numerical Analysis*, 26 (2006), 78–95.
[27] S. Mikhlin, *Variational methods in mathematical physics*, Pergamon, Oxford, 1964.
[28] S. Mikhlin, *Error Analysis in Numerical Processes*, Wiley and Sons, Chiester, New York, 1991.
[29] P. Neittaanmäki and S. Repin, *Reliable methods for computer simulation. Error control and a posteriori estimates*, Elsevier, New York, 2004.
[30] S. Repin, A posteriori error estimation for nonlinear variational problems by duality theory, *Zapiski Nauchnych Semin. POMI*, 243 (1997), 201–214.
[31] S. Repin, A posteriori error estimation for variational problems with uniformly convex functionals. *Math. Comp.*, 69 (2000), 481–500.
[32] S. Repin, A unified approach to a posteriori error estimation based on duality error majorants, *Mathematics and Computers in Simulation*, 50 (1999), 313–329.
[33] S. Repin, Two-sided estimates of deviation from exact solutions of uniformly elliptic equations. *Proceedings of the St. Petersburg Mathematical Society*, IX, 143–171, Amer. Math. Soc. Transl. Ser. 2, 209, 2003.
[34] S. Repin, S. Sauter and A. Smolianski, A posteriori error estimation for the Dirichlet problem with account of the error in the approximation of boundary conditions, *Computing*, 70 (2003), 205–233.
[35] C. Schwab, p- *and* hp- *Finite Element Methods*, Clarendon Press, Oxford, 1998.
[36] K. Shahbazi, An explicit expression for the penalty parameter of the interior penalty method, *Journal of Computational Physics*, 205 (2005), 401–407.
[37] S. Sun and M.F. Wheeler, $L^2\left(H^1\right)$ norm a posteriori error estimation for discontinuous Galerkin approximations of reactive transport problems, *Journal of Scientific Computing*, 22-23 (2005), 187–204.

[38] R. Verfürth, A posteriori error estimators for the Stokes equations, *Numer. Math.*, 55 (1989), 309–326.
[39] L.B. Wahlbin, *Superconvergence in Galerkin Finite Element Methods*, Lecture Notes in Mathematics, 1605, Springer-Verlag, 1995.
[40] O.C. Zienkiewicz and J.Z. Zhu, A simple error estimator and adaptive procedure for practical engineering analysis, *Int. J. Numer. Meth. Engrg.*, 24 (1987) 337–357.

Department of Mathematics, Texas A&M University, College Station, Texas 77843, U.S.A.
*E-mail address*: lazarov@math.tamu.edu

Laboratory of Mathematical Physics Petersburg Department of Steklov Institute of Mathematics 27, Fontanka, 191011, St.Petersburg, Russia
*E-mail address*: repin@pdmi.ras.ru

Johann Radon Institute for Computational and Applied Mathematics (RICAM), Austrian Academy of Sciences, Altenbergerstr. 69, A-4040 Linz, Austria
*E-mail address*: satyendra.tomar@ricam.oeaw.ac.at